Helmholtz-Zentrum Dresden-Rossendorf (HZDR)

HELMHOLTZ ZENTRUM
DRESDEN ROSSENDORF

Simulation of an MSLB scenario using the 3D neutron kinetic core model Dyn3D coupled with the CFD software Trio U

Grahn, A.; Gommlich, A.; Kliem, S.; Bilodid, Y.; Kozmenkov, Y.;

Originally published:

March 2017

Nuclear Engineering and Design 315(2017), 117-127

DOI: https://doi.org/10.1016/j.nucengdes.2017.02.002

Perma-Link to Publication Repository of HZDR:

https://www.hzdr.de/publications/Publ-24416

Release of the secondary publication
on the basis of the German Copyright Law § 38 Section 4.

CC BY-NC-ND

Simulation of an MSLB scenario using the 3D neutron kinetic core model Dyn3D coupled with the CFD software Trio_U

Alexander Grahn[1], André Gommlich, Sören Kliem, Yurii Bilodid, Yaroslav Kozmenkov

HZDR, Institute of Resource Ecology, Department of Reactor Safety, PB 510119, 01314 Dresden, Germany

Abstract

In the framework of the European project Nuresafe, the reactor dynamics code Dyn3D, developed at Helmholtz-Zentrum Dresden-Rossendorf (HZDR), was coupled with the Computational Fluid Dynamics (CFD) solver Trio_U, developed at CEA France, in order to replace Dyn3D's one-dimensional hydraulic part with a full three-dimensional description of the coolant flow in the reactor core at higher spatial resolution. The present document gives an introduction into the coupling method and shows results of its application to the simulation of an Main Steamline Break (MSLB) accident of a Pressurised Water Reactor (PWR).

1. Introduction

It is well known that the reactivity and the thermal power generation in the core of Light Water Reactors (LWRs) are very sensitive to changes in the feedback parameters moderator density and fuel temperature (Kliem et al., 2009). The latter is tightly connected to the moderator temperature and to the heat transfer between fuel and coolant, and thus strongly depends on the coolant flow conditions. Experimental and CFD analyses of the coolant flow in the Reactor Pressure Vessel (RPV) have shown that coolant mixing upstream of the core is highly incomplete (Moretti et al., 2008; Höhne et al., 2008; Höhne, 2009; Kliem et al., 2008), which may lead to large temporal and spatial gradients of temperature and boron in the core entry plane, especially in the case of cooling or boron dilution transients with asymmetric behaviour of the primary loops.

For the purpose of reactor safety assessment, a number of system codes, such as Athlet (Austregesilo et al., 2012), Cathare (Lavalle, 2006) and Relap5 (Nuclear Safety Analysis Division, 2001) have been developed. Being tools for whole-plant simulation, they cover virtually all key physical phenomena, but need to adopt various model simplifications in order to fulfill the intended task. They primarily focus on plant thermal-hydraulics while core physics (neutronics, core thermal-hydraulics and mechanics, fuel behaviour) rely on point kinetics and simplified fuel rod models. The ability for global plant analysis at relatively short computation times is bought with uncertainties that must be compensated by appropriate conservative assumptions.

During the past two decades, system codes have been integrated with core dynamics codes, like Dyn3D (Rohde et al., 2016) and Parcs (Downar et al., 2011), which solve the neutron diffusion equations in three spatial dimensions at higher resolution. Reactor core simulators like Dyn3D also involve the calculation of fuel burn-up, criticality, decay heat and thermal-mechanical fuel integrity and thus improve the accuracy and reliability of reactor safety analysis. Large effort has been put into the validation and verification of neutronic to thermal-hydraulic code couplings against plant transients and benchmark solutions, see e. g. (Mittag et al., 2001; Hämäläinen et al., 2002; Cuadra et al., 2004; Kliem et al., 2007; Agung et al., 2013; Kozmenkov et al., 2015).

[1]Corresponding author; mailto:a.grahn@hzdr.de

Reactor dynamics codes require the distributions of coolant velocity, temperature and boron at the core inlet as boundary conditions. These data can be provided by a thermal-hydraulic system code that calculates the redistribution of the coolant in the downcomer and in the lower plenum from loop data, using a low-resolution nodal representation of the RPV. Alternatively, a code like DYN3D may come with a built-in empirical model for coolant mixing (Kliem et al., 2004, 2006).

CFD methods are able to predict the coolant mixing in the RPV with higher accuracy than thermal-hydraulic codes and provide the core simulator with more realistic boundary conditions. In the framework of the NURESAFE project, the coupling of the three-dimensional CFD solver TRIO_U (Angeli et al., 2015) with the reactor core simulation programme DYN3D was implemented in order to improve the prediction of coolant mixing not only in the reactor downcomer and in the lower plenum, but also in the reactor core. In DYN3D, fuel assemblies are represented by one-dimensional coolant channels which are aligned with the vertical reactor axis. This prevents the code from reproducing lateral mixing across assembly boundaries. In order to remove this restriction, the three-dimensional CFD code TRIO_U was used to replace the core thermal-hydraulics of DYN3D.

2. The codes used in the coupling

2.1. Reactor dynamics code DYN3D

The reactor dynamics code DYN3D is a three-dimensional best-estimate tool for simulating steady states and transients of LWRs (LWRs) and has been developed at the HZDR, Germany, for more than 20 years. It is actively developed in order to improve the implemented and to embed new physical models and numerical methods. An in-depth introduction into DYN3D, the physical models it incorporates, its couplings with other thermal-hydraulic and fuel performance codes, as well as its applications is given in (Rohde et al., 2016; Bilodid et al., 2016). Therefore, only the most important features of DYN3D are summarized here.

The neutron kinetics model solves the three-dimensional neutron diffusion equations for two or multiple energy groups, or simplified neutron transport equations. Nodal expansion methods are applied that are specific for the geometry of fuel assemblies. Rectangular as well as hexagonal assembly shapes can be treated. The reactor is subdivided into axial layers of variable height, producing prismatic computational nodes which reflect the shape of the fuel assemblies. Recently, the solver was extended to trigonal prism nodes which allow the spatially refined nodalisation of hexagonal assemblies as well as the assignment of variable fuel compositions over the assemblies' cross section.

DYN3D includes a thermal-hydraulic model for one and two-phase coolant flow, and a fuel rod model. Thermal-hydraulic parameters like fuel and moderator temperatures are required for the estimation of safety criteria, such as the mechanical integrity of the fuel rods. On the other hand, together with the temperature dependent moderator density they are also needed for the determination of the feedback to neutronics. The thermal-hydraulic model solves the balance equations for mass, momentum and energy of the one or two-phase coolant flow, the heat transport equation in the fuel rod, and determines the heat transfer into the coolant. In an iterative procedure, DYN3D computes the distributions of fission power, coolant temperature and density, void fraction and boron concentration over the core, as well as safety-related parameters, such as maximum fuel and cladding temperatures, fuel enthalpy, critical heat flux and cladding oxide layer thickness.

Cross sections and other neutronic parameters are provided to the code in the form of libraries for different combinations of burnup and feedback parameters, and interpolated for each individual node and time step during a transient. Boundary conditions, like pressure drop over the core, boron concentration, coolant mass flow and coolant temperature distributions over the core inlet, are provided in the form of tables or by thermal-hydaulic codes coupled to DYN3D. Burnup distributions can be provided as input data or calculated by simulating power operation histories. Transient calculations may account for perturbations of the core inlet temperature, mass flow, boron concentration, outlet pressure, pressure drop and for control rod movement.

2.2. Fluid dynamics code TRIO_U

The code TRIO_U, recently renamed to TRIOCFD and put under the BSD license, is an

open-source, CFD simulation software, developed at CEA France. The code is designed to treat turbulent flows, fluid/solid coupling, multiphase flows (by means of front and particle tracking) or flows in porous media. Its parallelism allows the treatment of large three-dimensional problems, such as coolant flow in LWRs. TRIO_U calculates on structured (hexahedral) and un-structured (tetrahedral) meshes. Problem types that can be handled and which are relevant for LWR simulation comprise purely turbulent hydraulic as well as thermal-hydraulic problems with and without dissolved species transport.

For these problem types, TRIO_U solves the conservation equations of mass

$$\nabla \cdot \mathbf{u} = 0, \tag{1}$$

momentum

$$\frac{\partial \mathbf{u}}{\partial t} + (\mathbf{u}\cdot\nabla)\mathbf{u} = \frac{1}{\rho_{\mathrm{ref}}} \left\{ -\nabla p + \nabla \cdot \mu \left[\nabla \mathbf{u} + (\nabla \mathbf{u})^{\mathrm{T}} \right] \right\} + \left[1 - \beta_T (T - T_{\mathrm{ref}}) + \beta_C (C - C_{\mathrm{ref}}) \right] \mathbf{g}, \tag{2}$$

internal energy

$$\frac{\partial T}{\partial t} + \mathbf{u} \cdot \nabla T = \frac{1}{(\rho c_p)_{\mathrm{ref}}} \left[\nabla \cdot (\lambda \nabla T) + \dot{q}''' \right] \tag{3}$$

and dissolved species concentration

$$\frac{\partial C}{\partial t} + \mathbf{u} \cdot \nabla C = \nabla \cdot (D \nabla C). \tag{4}$$

For turbulent flows, equations for the turbulent kinetic energy and for the dissipation rate add to this list.

In this form, the equations imply the Boussinesq approximation, that is, the fluid density is assumed to have the constant value ρ_{ref} everywhere except in the body force term of the momentum equation. There, temperature and concentration dependency is represented by expansion coefficients β_T and β_C. Also, the specific heat capacity c_p is assumed to be constant.

3. Code coupling

3.1. Coupling method

For coupling DYN3D with TRIO_U an approach similar to a previous coupling effort based on the commercial CFD package ANSYS-CFX was adopted (Kliem et al., 2011; Grahn et al., 2015).

The part of DYN3D which solves the one-dimensional equations of momentum, boron and heat convection in a fuel assembly-wise manner is to be replaced by the fully three-dimensional simulation capabilities of TRIO_U. However, for the sake of acceptable computation times no attempt is made to model the coolant flow down to the fuel pin level. Instead, a porous body approach is used for modelling the reactor core. DYN3D computes the heat conduction in the fuel and the cladding, as well as the heat transfer into the coolant based on the coolant velocity which it receives from TRIO_U. For this purpose, DYN3D makes use of well-established correlations for the heat transfer at rod bundles that are implemented in its thermal-hydraulic module and which account for different heat transfer regimes occurring at heated surfaces.

The actual data interface between the codes is the volumetric heat source $\dot{q}'''$ in Eq. (3), calculated by DYN3D and sent to TRIO_U. In the opposite direction, boron concentration, coolant velocity v_z, temperature T and pressure p are sent to DYN3D. The quantities received from TRIO_U are needed to correctly calculate the neutronic feedback on nuclear power as well as the heat transfer into the coolant.

3.2. Coupling implementation

On the coding level, the coupling of DYN3D and TRIO_U makes use of the SALOMÉ platform (`http://www.salome-platform.org`). It is an open-source software for pre and post processing numerical simulations as well as a programming framework for the integration and coupling of third-party simulation codes based on open standards. For the purpose of code coupling it provides programming classes and methods for data storage, data interpolation and the generation of computational meshes.

In order to communicate with each other, the simulation codes to be coupled must implement a common programming interface. For this, SALOMÉ defines ICOCO which stands for Interface for Code Coupling. (Deville and Perdu, 2012). It is a purely abstract C++ programming interface to be implemented in the codes. Every code is represented by an object of type `Problem` whose methods allow a supervising programme to initialise and terminate

the code, to increment the problem time, to invoke the solution of a time step, to extract solution fields from the code and to send fields to the code.

The supervisor programme is responsible for the creation of class instances, also known as objects, of type `Problem`, where each object represents one of the coupled codes. In the case of parallel execution, each code instance is represented by a separate object. Codes working in parallel communicate through channels provided by the Open MPI library (`http://www.open-mpi.org`) which have to be created and passed to the `Problem` instances by the supervisor upon initialization. Moreover, the supervisor takes charge of time advancing and data interpolation which are performed totally outside the coupled codes.

In general, Dyn3D and Trio_U work on computational meshes of different spatial resolution. In order to interpolate the solution fields between the coarse Dyn3D and the refined and possibly partitioned Trio_U mesh, the supervisor makes use of an interpolation class which is also provided by Salomé and which is closely integrated with the Open MPI parallelization library. The interpolation class implementation of Salomé ensures the conservation of the interpolated quantity as well as the fulfilment of the maximum principle during interpolation. Fig. 1 sketches the coupling between Dyn3D and Trio_U and shows the exchanged quantities.

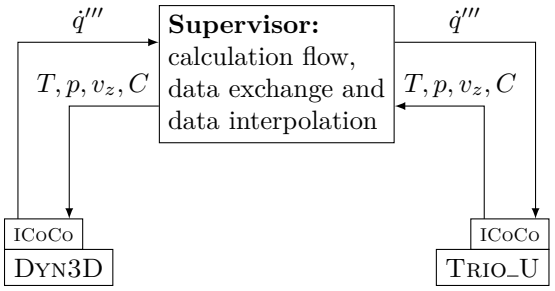

Figure 1: Coupling scheme and quantities transferred between Dyn3D and Trio_U

The supervisor programme implements an explicit time-stepping scheme, that is, Dyn3D and Trio_U advance by the same time step Δt and the exchange of solution fields takes place once at the start of a new step. The coupling algorithm is shown in Fig. 2.

After start, the supervisor creates the `Problem` objects of Dyn3D and of every parallel Trio_U process. (Currently, Dyn3D is a single-threaded application. Its parallelization is being implemented.) It should be noted that Dyn3D and Trio_U are not used in their standalone versions. In coupling applications they are loaded from shared libraries where they are packaged together with the ICoCo wrappers. The code instances are instructed to read their respective set-up files. Afterwards, interpolation objects are created for every quantity to be exchanged.

The solution of a new time step begins with the determination of a suitable time step width Δt by selecting the minimum value out of the values delivered by all involved code instances, including the parallel Trio_U instances. Selecting the minimal time step width ensures stable convergence during the simulation run. The parallelization of Trio_U is based on partitioning the mesh of the computational domain according to the number of available CPUs. The optimal Δt depends on local coolant velocities and mesh resolution and is computed according to the Courant-Friedrichs-Lewy criterion. Since Trio_U operates on a higher mesh resolution as compared to Dyn3D, one of the Trio_U instances usually requests the smallest Δt value. After retrieving the solution fields from the sending code instances and their interpolation onto the meshes of the receiving codes, the solution of the new time step is carried out. The problem time is incremented and if the end of the transient has not been reached, the programme flow loops back to finding the next Δt.

4. Verification

4.1. Test case

The implementation of the code coupling is verified by comparing the coupled simulation result of a control rod insertion transient with the standalone Dyn3D calculation.

The transient starts from the stationary state of a Konvoi-type PWR, consisting of 193 fuel assemblies, at hot full power with a nominal thermal power of 3500 MW. The burn-up state of the core corresponds to the beginning of an equilibrium fuel cycle. The core is fed with a coolant mass flow of $18\,596\,\mathrm{kg\,s^{-1}}$ at a temperature of 280 °C and with a boron concentration of 1363 ppm; the pressure of 15.8 MPa prevails at the top of the core.

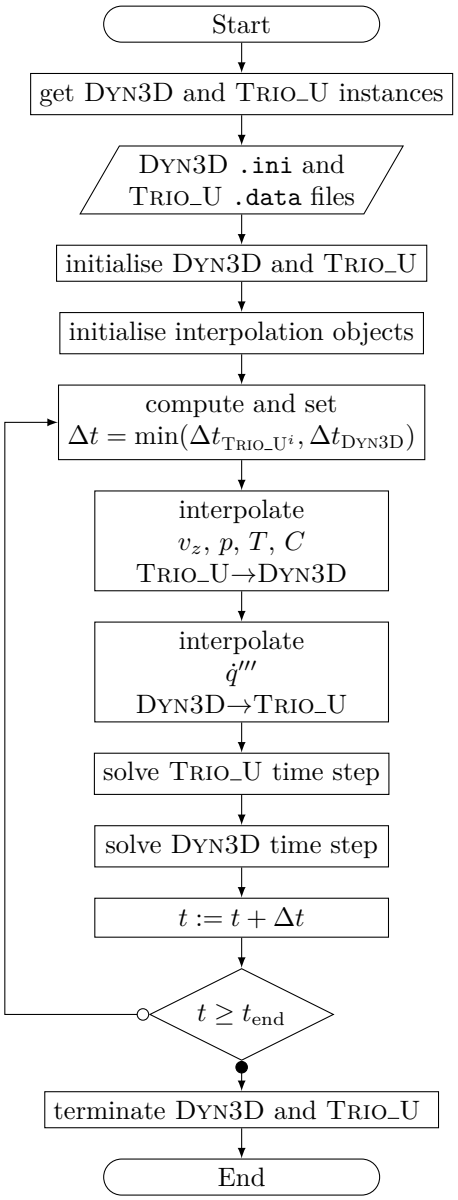

Figure 2: Flow diagram of the coupling supervisor programme

During the transient, all control rods of the reactor are moved at constant speed into the core. This procedure starts at $t = 1\,\text{s}$ and takes 10 s to accomplish until the rods have been fully inserted.

The Dyn3D domain is spatially discretized into 14 equally-sized nodes per fuel assembly which corresponds to a total of 2702 nodes. The Trio_U domain is divided into 228 tetrahedral mesh cells per Dyn3D node amounting to 778176 cells in the whole reactor core. At the beginning of the simulation, an initial time step Δt of 0.001 s was chosen which was automatically adjusted later to meet the stability requirements of each code involved.

Fig. 3 plots the total power of the core over time. The coupled simulation and the Dyn3D standalone result agree very well. However, there is a steeper increase of the temperature along the assembly height in the case of the coupled simulation as compared to the standalone result, Fig. 4. Within the temperature range occurring between the core inlet and outlet, the change of the specific heat capacity c_p and of the coolant density ρ cannot be neglected, and the assumption of constant material properties, as implemented in Trio_U, is not justified anymore. Between 280 °C and 340 °C, c_p of the coolant increases from 5.06 to 7.83 $\text{kJ kg}^{-1}\,\text{K}^{-1}$ and the density falls from 765 to 617 kg m^{-3}. The combined quantity (ρc_p), i. e. the volumetric heat capacity, increases by a factor of 1.25 between core inlet and outlet. The Trio_U part of the test case was configured to use material properties ρ_{ref}, $c_{p_{\text{ref}}}$ which correspond to the inlet condition at 280 °C. Hence, the lower volumetric heat capacity value at that temperature was used in the whole core which led to the higher temperature at the core outlet.

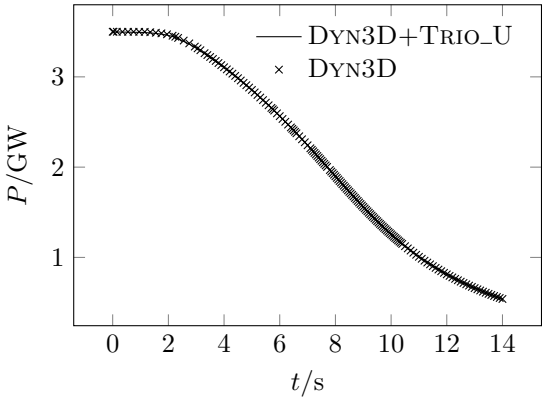

Figure 3: Total reactor power during control rod insertion transient; comparison of coupled and Dyn3D-standalone calculations

4.2. Modified heat source

The discrepancies that are observed when comparing the Dyn3D standalone and the coupled Dyn3D/Trio_U calculation results are mainly

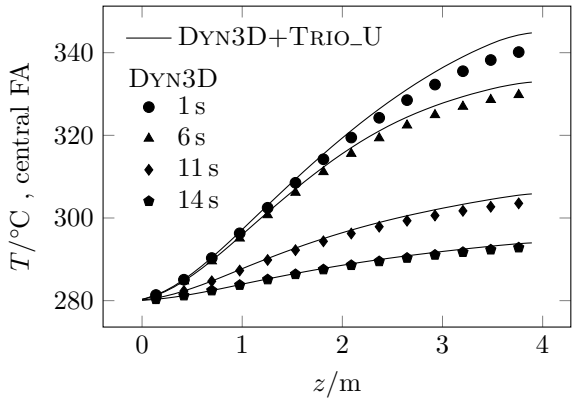

Figure 4: Coolant temperature profiles along the central fuel assembly at different times of control rod insertion transient; comparison of coupled and Dyn3D-standalone calculations

caused by the Boussinesq approximation used in Trio_U. At least for the heat source term $\dot{q}'''$ in the internal energy equation Eq. (3), this approximation can be worked around. Since Trio_U exposes $\dot{q}'''$ as an input variable for the purpose of code coupling, it can be written to with distributions from external sources. By suitably scaling the heat source obtained from Dyn3D, the effect of the volumetric heat capacity whose reference value $(\rho c_p)_{\mathrm{ref}}$ turns out to be too small in the hotter core regions can be compensated. The modified heat source reads

$$\dot{q}'''^{*} = \frac{(\rho c_p)_{\mathrm{ref}}}{(\rho c_p)_T} \dot{q}'''. \tag{5}$$

The power density $\dot{q}'''$, as supplied by Dyn3D, is first interpolated onto the refined Trio_U mesh and then scaled by the factor $(\rho c_p)_{\mathrm{ref}}/(\rho c_p)_T$. The local values of $(\rho c_p)_T$ on the Trio_U mesh are calculated from the coolant temperature distribution that Trio_U outputs at every time step and using the IFC-67 formulation of water/steam properties.

Fig. 5 shows the result of a simulation which uses the new heat source $\dot{q}'''^{*}$ in the Trio_U part. Good agreement between the coupled and the standalone Dyn3D simulations can now be observed, in particular during the early phase (1 s, 6 s) of the transient where large temperature gradients prevail along the assembly height. At later stages, a slight overestimation of coolant temperature can sill be observed. Other effects which are not directly related to the heat capacity are more important here. For example, in the continuity equation (1), the Boussinesq approximation neglects the coolant expansion caused by heating. This leads to an underestimation of the coolant velocity which in turn affects the heat transfer from the fuel rod surface to the coolant and prolongs the contact time between the coolant and the heated core. Since there is no direct access to the equations solved in Trio_U such effects cannot be compensated.

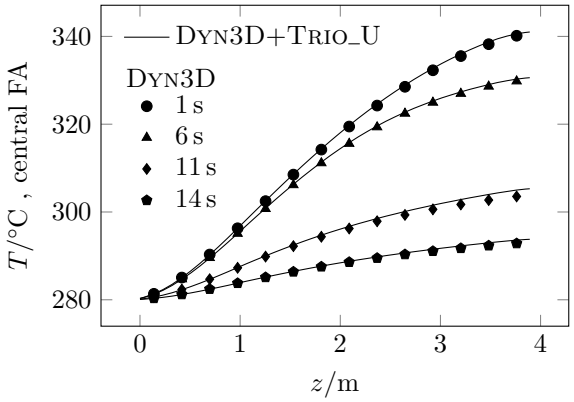

Figure 5: Coolant temperature profiles along the central fuel assembly based on the modified heat source, Eq. (5); comparison of coupled and Dyn3D-standalone calculations

5. MSLB simulation

The transient response of a light water reactor to a secondary-side steam line break was simulated using the newly developed coupling between Trio_U and Dyn3D. The computational domain comprises the RPV with its four inlet nozzles of the corresponding primary coolant loops, the downcomer, the lower plenum up to the core inlet plane, and the reactor core up to the core outlet plane. In that way, all parts of the primary circuit, where 3D coolant mixing effects are important in such scenarios are included into the computational domain. Time-dependent boundary conditions at the nozzle inlet (coolant mass flow, temperature, boron concentration) are provided as tabulated input data and were generated by prior system-code calculations.

5.1. Computational domain

In Fig. 6a and b, the computational geometries of the RPV and of the reactor core are shown as

surface meshes, while Fig. 6c is a sectional view of the entire computational mesh in the vertical plane of the loop 1 and 3 inlet nozzles. Two separate, unstructured meshes composed of tetrahedral cells are used to model the reactor in the CFD calculation done by TRIO_U. At their connecting faces, which lie in the plane of the core inlet, the two meshes are non-conforming. That means, the two mesh surfaces being brought into contact while connecting both geometries are not congruent. This requires interpolation of the quantities to be transferred at this internal boundary. Therefore, two separate TRIO_U problem instances, one for each subdomain, are created and coupled which each other in the supervisor programme. This is done in a similar way as for the TRIO_U-DYN3D coupling in the reactor core. However, only two-dimensional distributions of pressure, velocity, temperature and concentration need to be interpolated and transferred between the simulation parts. Thus, the whole simulation set-up is a triple coupling between two TRIO_U instances for simulating the coolant flow in the upstream RPV part and in the reactor core, and one DYN3D instance for the neutronic simulation of the core.

DYN3D calculates on a low-resolution nodal mesh which is shown in Fig. 6d. It divides the reactor core into 32 layers between inlet and outlet, while every fuel assembly is represented by one node horizontally, giving a total of $32 \times 193 = 6176$ nodes. The refined core mesh, Fig. 6b, used in the CFD calculation is obtained by subdividing every node of the DYN3D core mesh into three layers in the vertical direction and into four cells horizontally. This produces $4 \times 3 \times 6176 = 74\,112$ hexahedral cells which in turn are cut along the surface diagonals. This produces 24 tetrahedra per cell and a total of $24 \times 74\,112 = 1\,778\,688$ tetrahedra in the whole reactor core domain. The RPV mesh, Fig 6a, contains 1 906 272 tetrahedral cells. Fig. 7 illustrates the refinement procedure.

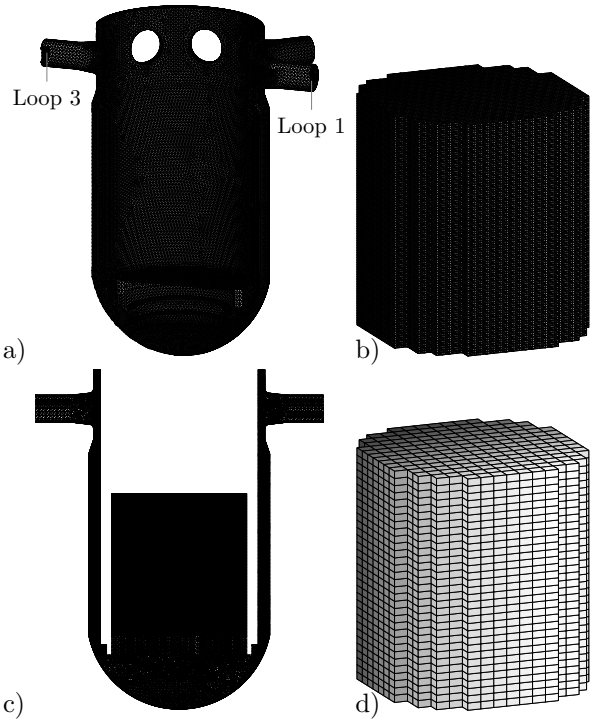

Figure 6: Mesh geometries for the coupled DYN3D-TRIO_U simulation; a) RPV model in TRIO_U (partial surface mesh), b) reactor core model in TRIO_U, c) vertical section of the TRIO_U mesh in the plane of loop 1 and loop 3 inlet nozzles, d) reactor core nodal mesh for DYN3D

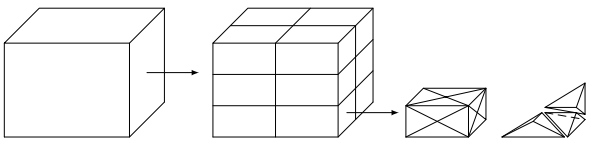

Figure 7: Refinement of a DYN3D hexahedral node into multiple tetrahedra of the TRIO_U mesh

5.2. Problem specification

The reference reactor is a 4-loop PWR of Westinghouse design whose core configuration and materials composition is given in (Kozlowski and Downar, 2003). At the beginning of the transient, the core is at end-of-cycle and hot-zero power, with zero boron concentration in the primary coolant and zero decay heat power. The total coolant mass flow amounts to $17\,346\,\mathrm{kg\,s^{-1}}$, equally distributed between the four loops. The primary loop coolant temperature is 283.8 °C and the pressure at the reactor outlet is 15.4 MPa. The two-group homogenized cross-sections library for the transient simulation was generated by Sanchez-Cervera et al. (2014) in NEMTAB multi-dimensional table format using APOLLO II (Sanchez et al., 1988) lattice physics code utilizing 281-group neutron data library based on JEFF3.1.1. (Koning et al., 2010) and was connected to the problem in the same way as in the boron dilution analyses reported in (Jimenez et al., 2015).

The transient is initiated by a double-ended MSLB at the outlet nozzle of the steam generator in loop 1. This leads to a sudden evaporation of secondary coolant and thus to a strong temperature drop of the secondary coolant. As the temperature difference between the primary and the secondary sides of the steam generator increases, more heat is removed from the primary coolant which causes the primary loop temperature to also drop. As a consequence, the reactor core suffers an overcooling, which causes it to become critical and to produce a power excursion. To increase the power generation during the transient and to achieve an additional asymmetry in the core a fuel assembly with a stuck control rod was assumed. The rod is completely outside of the core. The assembly position, as shown in Fig. 8, was chosen to be in the same sector of the core which is also expected to be most affected by the overcooling originating from loop 1.

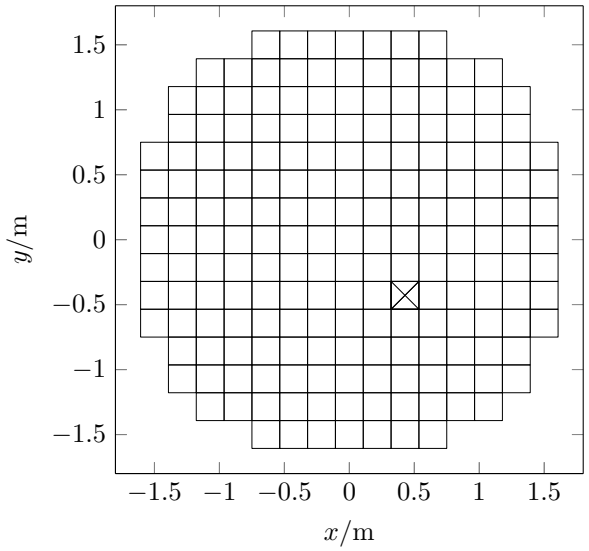

Figure 8: Position (⊠) of the fuel assembly with stuck control rod

Various countermeasures are aimed at readjusting the secondary side pressure and the primary coolant temperatures in order to bring the reactor core back to the sub-critical state. All primary coolant pumps remain in operation, providing the core with a nearly constant feed of coolant, cf. Fig. 9a. Fig. 9b shows the primary coolant temperatures at the RPV inlet nozzles during the transient. Together with the volumetric flow rates, Fig. 9a, they represent the inlet boundary conditions for the coupled simulation.

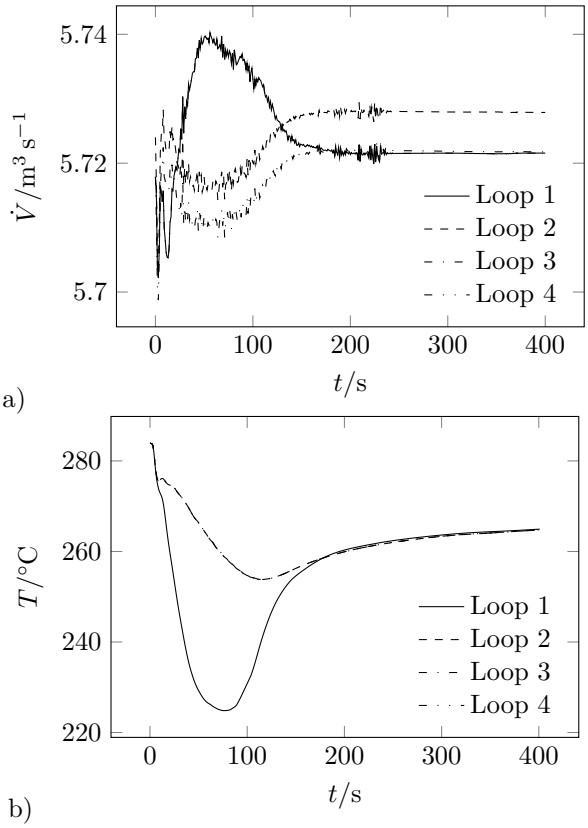

Figure 9: Volumetric flow rate (a) and temperature (b) at the cold legs of the primary coolant loops during MSLB transient

5.3. Simulation results

According to Fig. 9, the maximum overcooling by about 60 K is reached after 76 s. The response of the thermal power to the overcooling transient is shown in Fig. 10. The power reaches the peak after 92 s with a delay of 16 s as compared to the minimum coolant temperature of loop 1. It starts to drop as the coolant temperatures grow in all primary loops.

Coolant mass flow densities in the vertical direction at the core inlet level are shown in Fig 11. Unlike the cold leg positions, the maxima of the downward flow (shaded dark) in the annular gap are separated by quarter circles, approximately. Interestingly, loop 1 and 3 coincide with the minima

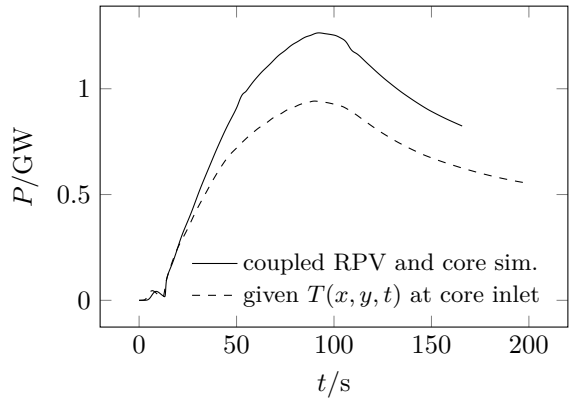

Figure 10: Reactor power during MSLB transient, comparison of coupled RPV/core simulation and core-only simulation with given core inlet temperature distribution

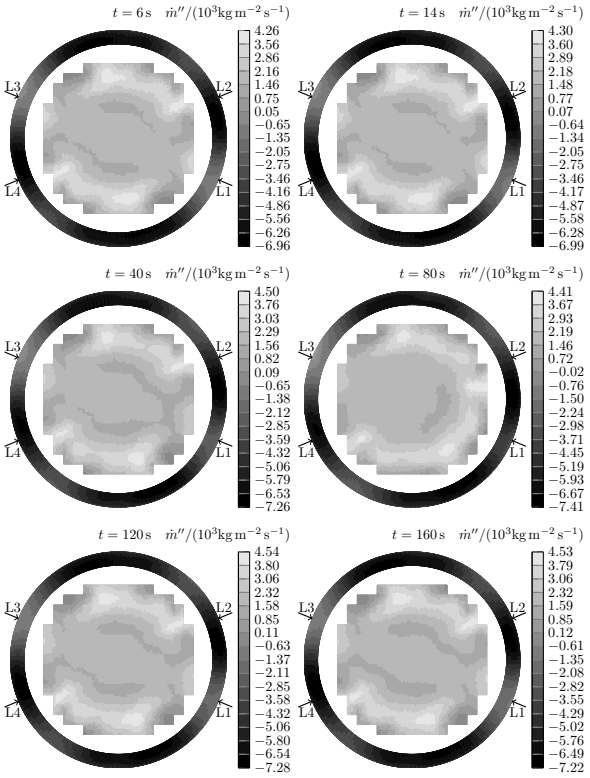

Figure 11: Coolant mass flow densities in z direction at the core inlet level; arrows indicating the cold leg nozzle positions

(shaded bright) of the downward flow, although, even at the beginning ($t = 6\,\mathrm{s}$), mass flow rates are the same in all loops. According to the simulation, the mass flow density is fairly unevenly distributed across the core inlet. The maximum upward flow (shaded bright) is localized in the outer core region, but does not form a closed annulus. Instead, it is interrupted by a belt of low mass flow extending diagonally across the core cross section between the loop 1 and 3 inlet nozzle positions. Small, constricted areas with a mass flow density close to zero exist in the outermost zone of the core cross section.

Temperature distributions over two cross sections of the core, namely at the inlet and the outlet positions, are shown in Fig. 12. Up to the first 6 seconds of the simulated transient, the overcooling is the same for all loops, cf. Fig. 9b, and the inlet temperature distribution resembles the mass flow density distribution, cf. Fig. 11, in that the outer zone of the core is more affected by overcooling than its centre and that there is a diagonal band with little overcooling. As time advances, temperature differences between hotter and overcooled zones grow and a sector of overcooling forms around the loop 1 inlet position in the core inlet plane. Later on, as it can be seen for $t = 160\,\mathrm{s}$, this overcooling sector vanishes again because the inlet temperatures of all loops start to approach each other after the passage of the minimum temperature, cf. Fig 9b. In the outlet plane, beginning at $t = 14\,\mathrm{s}$, a spot of elevated coolant temperature forms around the position of the assembly with the stuck control rod. Fig. 13 shows the power density distribution in a plane cutting the core vertically along the core axis and the centre line of the affected assembly. During the transient, starting at zero, the power density reaches values beyond $200\,\mathrm{MW\,m^{-3}}$. Despite the high energy release in the affected assembly during the power peak at $t = 92.5\,\mathrm{s}$, the coolant passing throught it only reaches temperatures around 285 °C, cf. Fig. 14, which is similar to the stationary state value. The temperature jump with respect to the minimum inlet temperature of loop 1 is about 60 K. Fig. 14 also shows the power density profile in the affected assembly during the core power peak. Its steplike profile is due to the fact, that the power density distribution is calculated by Dyn3D on the coarse nodal mesh.

Based on coolant mixing tests at the Rocom facility (Höhne et al., 2008; Kliem et al., 2010),

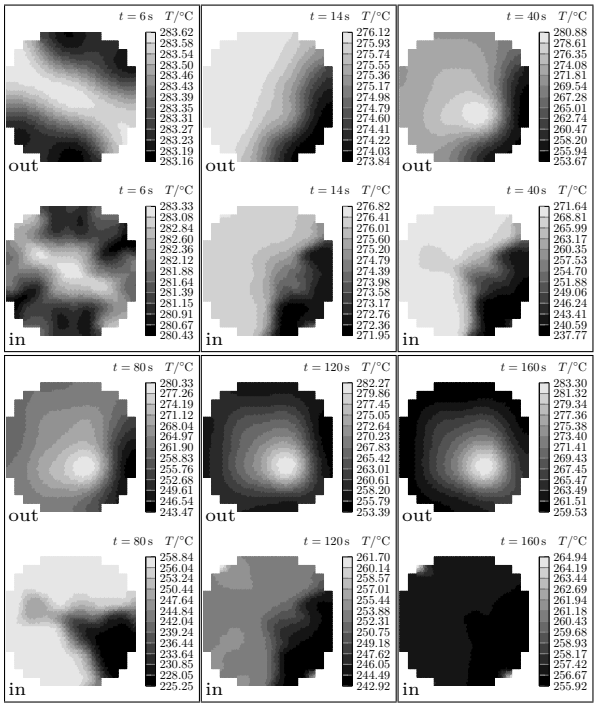

Figure 12: Core inlet (in) and outlet (out) temperature distributions at different times

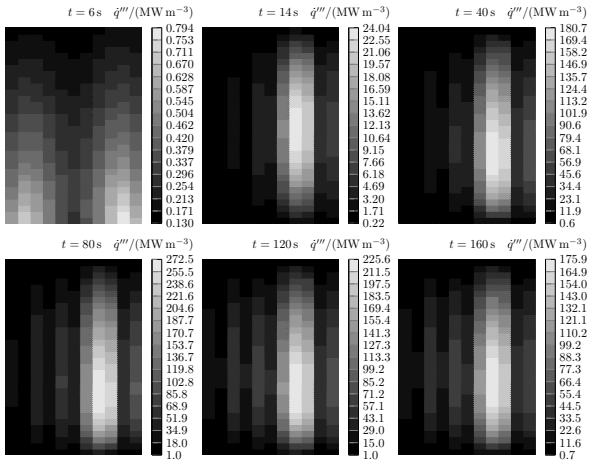

Figure 13: Power density distribution in the vertical plane $x + y = 0$ at different times

an MSLB simulation was carried out which uses a time-dependent coolant temperature distribution over the core inlet plane as the upstream boundary condition. The ROCOM facility is a downscaled RPV model of a KONVOI reactor, instrumented with conductivity measurement technique, that was

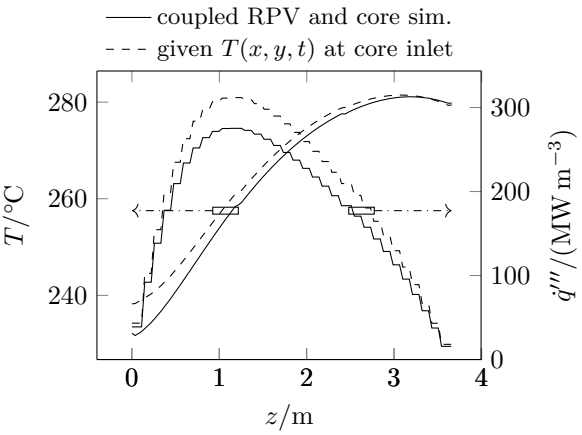

Figure 14: Profiles of coolant temperature and power density along the fuel assembly with stuck control rod at $t = 92.5\,\mathrm{s}$, comparison of coupled RPV/core simulation and core-only simulation with given core inlet temperature distribution

mainly used to investigate the coolant mixing behaviour upstream of the core zone. The tests cover a number of transient scenarios with single and multiple loop flow rate and concentration variations. The measured mixing scalar distribution of a test with single-loop disturbance was scaled onto the MSLB conditions of the present study. The following comparison case with core-only simulation uses the same total coolant flow rate, but unlike the full-RPV simulation presented before, it assumes a uniform flow rate over the core inlet during the transient. Thus, the comparison case serves to investigate the effect of a non-uniform coolant flow at the core inlet on the overall reactor power and the resulting coolant temperature. Distributions of coolant temperature at the core inlet and outlet are shown in Fig. 15. The inlet temperature distributions, marked with (in), as provided by the experiment, appear more regularly shaped and smoother than those obtained in the previous full-RPV simulation and the difference between minimum and maximum values is smaller, most prominently at $t = 160\,\mathrm{s}$. The total thermal reactor powers of the two cases are plotted against each other in Fig. 10. The power maximum, occurring around the same time as in the full-RPV case, is by about 0.3 GW lower (dashed curve). On the other hand, on the local level, power density and coolant temperature are higher in the core-only simulation, as can be seen in Fig. 14 showing the vertical profiles in the

assembly with a stuck rod around the time of the power maximum. From comparing the two simulation cases it can be concluded that the vessel built-ins, e. g. the perforated drum in the lower plenum, have a levelling effect on the coolant flow and tempereature fields which are not fully reproduced by CFD in the full-RPV simulation.

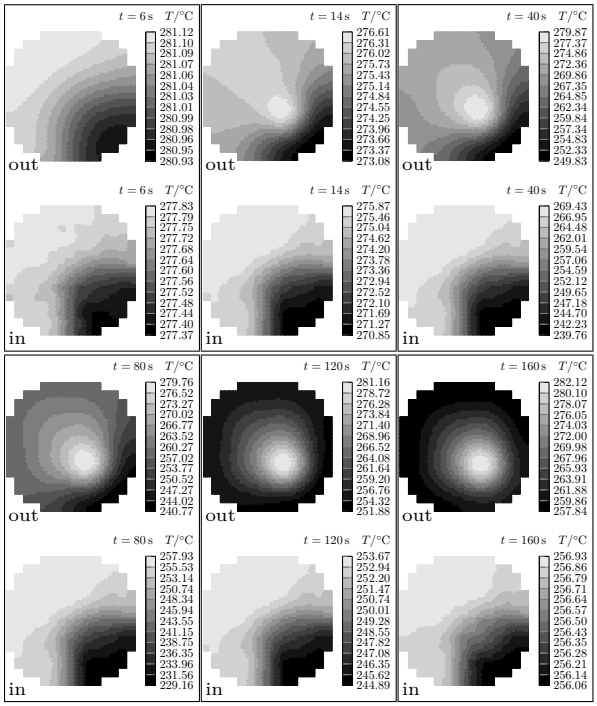

Figure 15: Core inlet (in) and outlet (out) temperature distributions at different times; comparison case with core-only simulation and given $T(x, y, t)$ core inlet

One interesting feature of the temperature profile in Fig. 14 is the slight decrease in the upper section of the assembly above $z = 3\,\mathrm{m}$. This can be explained only by lateral mixing with colder water from the neighbourhood of the affected assembly. Indeed, as can be observed in Fig. 16, horizontal velocity components are non-zero in the upper part close to the core outlet, which is a precondition for lateral mixing. The presence of horizontal velocity proves the existence of three-dimensional coolant flow in the reactor core which cannot be modelled by standalone Dyn3D.

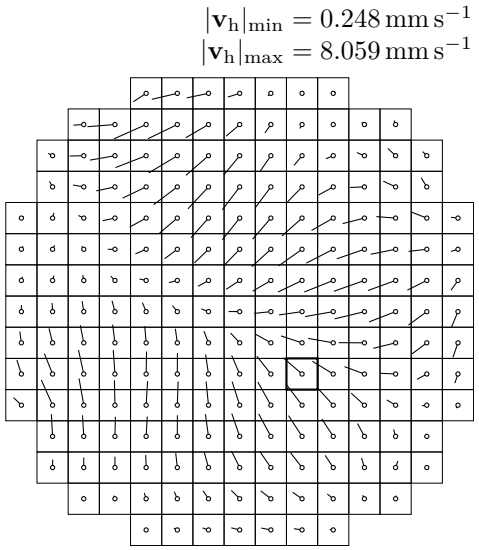

Figure 16: Distribution of horizontal coolant velocity components $\mathbf{v}_\mathrm{h} = (v_x, v_y)$ close to the core outlet at $t = 92.5\,\mathrm{s}$

6. Conclusions

The CFD code Trio_U has been coupled with the reactor dynamics code Dyn3D in order to replace its one-dimensional description of the core thermal-hydraulics with a fully three-dimensional simulation of the coolant flow and temperature fields on a refined grid. Coolant velocity, pressure, temperature and boron concentration fields are calculated by Trio_U and sent to Dyn3D which calculates the core power density distribution. The latter is sent back to the CFD code and used there as a source term in the solution of the energy transport equation. Data storage and interpolation make use of the facilities provided by Salomé, an open-source platform for simulation code integration. The object oriented libraries of the platform are closely integrated with the Open MPI parallelization library and are fully compatible with the parallelism of Trio_U.

The code coupling was verified against a standalone Dyn3D simulation of a control rod insertion transient of a pressurized reactor core. The simulation error caused by the Boussinesq approximation in Trio_U could be partly compensated by modifying the Dyn3D-provided power density. Good agreement could be achieved between the coupled and the standalone simulations, but the applicability of the coupling remains limited to cases with

mild coolant temperature changes in space and time.

A triple coupling of two TRIO_U and one DYN3D instances was implemented to also simulate the coolant mixing in the RPV upstream of the core inlet plane. This coupling was applied to an MSLB case which involves an overcooling transient in a single loop of the primary circuit. The simulation confirmed the incomplete mixing in the downcomer and the lower plenum leading to a sector-shaped distribution of the coolant temperature in the core inlet plane. Moreover, the simulation produced a three-dimensional flow field in the reactor core, which leads to lateral mixing of coolant on its passage through the core.

Acknowledgements

The presented work was financed by the European Union within the FP7 NURESAFE project.

The authors would like to express their sincere gratitude to Mme Céline Capitaine from the TRIOCFD development and support team at CEA France for her swift and thorough help with all aspects of TRIO_U, including difficult low-level programming issues that the authors faced during their work on the code coupling. Furthermore, the authors thank Ladislav Vyskočil from ÚJV Řež, Czech Republic, for providing the computational mesh of the RPV.

References

Agung, A., et al., 2013. Validation of PARCS/RELAP5 coupled codes against a load rejection transient at the Ringhals-3 NPP. Nuclear Engineering and Design 257, 31–44.

Angeli, P.-E., Bieder, U., Fauchet, G., 2015. Overview of the TrioCFD code: main features, v&v procedures and typical applications to nuclear engineering. In: NURETH-16.

Austregesilo, H., et al., 2012. ATHLET Mod. 3.0 Cycle A Models and Methods. GRS, GRS–P–1, vol. 4 rev. 3.

Bilodid, Y., Kotlyar, D., Shwageraus, E., Fridman, E., Kliem, S., 2016. Hybrid microscopic depletion model in nodal code DYN3D. Annals of Nuclear Energy 92, 397–406.

Cuadra, A., et al., 2004. Analysis of a Main-Steam-Line Break in Asco NPP. Nuclear Technology 146.

Deville, E., Perdu, F., 2012. Documentation of the Interface for Code Coupling: ICoCo. CEA, Paris.

Downar, T., et al., 2011. PARCS v2.6 U.S. NRC Core Neutronics Simulator Theory Manual. Purdue University.

Grahn, A., Kliem, S., Rohde, U., 2015. Coupling of the 3D neutron kinetic core model DYN3D with the CFD software ANSYS-CFX. Annals of Nuclear Energy 84, 197–203.

Hämäläinen, A., Kyrki-Rajamäki, R., Mittag, S., Kliem, S., Weiß, F.-P., Langen-buch, S., Danilin, S., Hádek, J., Hegyi, G., 2002. Validation of coupled neutron kinetic/thermal-hydraulic codes Part 2: Analysis of a VVER-440 transient (Loviisa-1). Annals of Nuclear Energy 29, 255–269.

Höhne, T., 2009. CFD-simulation of the VVER thermal hydraulic benchmark V1000CT-2 using ANSYS-CFX. Science and Technology of Nuclear Installations 2009.

Höhne, T., Kliem, S., Rohde, U., Weiss, F.-P., 2008. Boron dilution transients during natural circulation flow in PWR—Experiments and CFD simulations. Nucl. Eng. Design 238, 1987–1995.

Jimenez, G., Herrero, J., Gommlich, A., Kliem, S., Cuervo, D., Jimenez, J., 2015. Boron dilution transient simulation analyses in a PWR with neutronics/thermal-hydraulics coupled codes in the NURISP project. Annals of Nuclear Energy 84, 86–97.

Kliem, S., Danilin, S., Hämäläinen, A., Hádek, J., Keresztúri, A., Siltanen, P., 2007. Qualification of coupled 3D neutron kinetic/thermal hydraulic code systems by the calculation of main steam line break benchmarks in a NPP with VVER-440 reactor. Nuclear Science and Engineering 157, 280–298.

Kliem, S., Gommlich, A., Grahn, A., Rohde, U., Schütze, J., Frank, T., Gomez, A., Sanchez, V., 2011. Development of multi-physics code systems based on the reactor dynamics code DYN3D. Kerntechnik 76, 160–165.

Kliem, S., Höhne, T., Rohde, U., Weiss, F.-P., 2010. Experiments on slug mixing under natural circulation conditions at the ROCOM test facility using high resolution measurement technique and numerical modeling. Nucl. Eng. Design 240, 2271–2280.

Kliem, S., Kozmenkov, Y., Höhne, T., Rohde, U., 2006. Analyses of the V1000CT-1 benchmark with the DYN3D/ATHLET and DYN3D/RELAP coupled code systems including a coolant mixing model validated against CFD calculations. Progress in Nuclear Energy 48, 830–848.

Kliem, S., Mittag, S., Rohde, U., Weiß, F.-P., 2009. ATWS analysis for PWR using the coupled code system DYN3D/ATHLET. Annals of Nuclear Energy 36, 1230–1234.

Kliem, S., Rohde, U., , Weiss, F.-P., 2004. Core response of a PWR to a slug of under-borated water. Nuclear Engineering and Design 230, 121–132.

Kliem, S., Sühnel, T., Rohde, U., Höhne, T., Prasser, H.-M., Weiss, F.-P., 2008. Experiments at the mixing test facility ROCOM for benchmarking of CFD-codes. Nucl. Eng. Design 238, 566–576.

Koning, A. J., et al., 2010. Status of the JEFF Nuclear Data Library. In: Proceedings of the International Conference on Nuclear Data for Science and Technology. Jeju Island, Korea, p. 1057.

Kozlowski, T., Downar, T. J., 2003. OECD/NEA and US NRC PWR MOX/UO_2 core transient benchmark, final specifications, Rev. 2. Tech. Rep. NEA/NSC/DOC(2003)20, NEA.

Kozmenkov, Y., Kliem, S., Rohde, U., 2015. Validation and verification of the coupled neutron kinetic/thermalhydraulic system code DYN3D/ATHLET. Annals of Nuclear Energy 84, 153–165.

Lavalle, G., 2006. CATHARE V2.5.1: User's manual. CEA.

Mittag, S., Kliem, S., Weiß, F.-P., Kyrki-Rajamäki, R., Hämäläinen, A., Langenbuch, S., Danilin, S., Hádek, J., Hegyi, G., Kuchin, A., Panayotov, D., 2001. Validation of coupled neutron kinetic/thermal-hydraulic codes Part 1: Analysis of a VVER-1000 transient (Balakovo-4). Annals of Nuclear Energy 28, 857–873.

Moretti, F., Melideo, D., D'Auria, F., Höhne, T., Kliem, S., 2008. CFX Simulations of ROCOM Slug Mixing Experiments. Journal of Power and Energy Systems 2 (2), 720–733.

Nuclear Safety Analysis Division, 2001. RELAP5/MOD3.3 code manual. U. S. Nuclear Regulatory Commission, NUREG/CR-5535/Rev 1.

Rohde, U., et al., 2016. The reactor dynamics code DYN3D—models, validation and applications. Progress in Nuclear Energy 89, 170–190.

Sanchez, R., et al., 1988. APOLLO II: a user-oriented, portable, modular code for multigroup transport assembly calculations. Nucl. Sci. Eng. 100, 352–362.

Sanchez-Cervera, S., Garcia-Herranz, N., Bernard, F., 2014. Nodal-level XS library parameterized for MSLB. Tech. Rep. NURESAFE deliverable D12.23, European Commission.